Research Article | Vol. 25, No. 13 | 26 Jun 2017 | OPTICS EXPRESS 14795

Optics EXPRESS

Low aberration and fast switching microlenses based on a novel liquid crystal mixture

JOSÉ FRANCISCO ALGORRI,[1,*] NOUREDDINE BENNIS,[2] JAKUB HERMAN,[3] PRZEMYSLAW KULA,[3] VIRGINIA URRUCHI,[1] AND JOSÉ MANUEL SÁNCHEZ-PENA[1]

[1]*Department of Electronic Technology, Carlos III University, Madrid 28911, Spain*
[2]*Institute of Applied Physics, Military University of Technology, Warsaw 00-908, Poland*
[3]*Institute of Chemistry, Military University of Technology, Warsaw 00-908, Poland*
[*]*jalgorri@ing.uc3m.es*

Abstract: In this work, we present a novel kind of LC mixture (5005) for photonic applications, with emphasis on a LC microlens array. This mixture is a nematic composition of three different families of rod like liquid crystals. The key is that frequency dependence of parallel component of electric permittivity is different for each component, resulting in a strongly dependent on frequency dielectric anisotropy. The unique properties of this LC mixture are demonstrated to work in a frequency modulated LC microlens array. A hole patterned structure is used. Thanks to the special characteristics of this mixture, the microlenses are reconfigurable by low voltage signals with variable frequency. This is a first demonstration of a LC lens with tunable focal length by frequency in an analog way. The result of this type of control are microlenses with low aberrations and fast switching (the frequency switching is around 10 times faster than amplitude modulation). The tunability with frequency and the fast switching, makes this liquid crystal of special interest not only for microlenses but for all kind of optical phase modulators.

OCIS codes: (250.0250) Optoelectronics; (230.3720) Liquid-crystal devices; (230.4110) Modulators.

References and links

1. G. E. Nevskaya and M. G. Tomilin, "Adaptive lenses based on liquid crystals," J. Opt. Tech. **75**(9), 563–573 (2008).
2. J. F. Algorri, V. Urruchi, B. Garcia-Cámara, and J. M. Sánchez-Pena, "Liquid crystal lensacons, logarithmic and linear axicons," Materials (Basel) **7**(4), 2593–2604 (2014).
3. J. F. Algorri, V. Urruchi, N. Bennis, and J. M. Sánchez-Pena, "Modal liquid crystal microaxicon array," Opt. Lett. **39**(12), 3476–3479 (2014).
4. J. F. Algorri, G. D. Love, and V. Urruchi, "Modal liquid crystal array of optical elements," Opt. Express **21**(21), 24809–24818 (2013).
5. J. F. Algorri, V. Urruchi, B. Garcia-Camara, and J. M. Sánchez-Pena, "Generation of optical vortices by an ideal liquid crystal spiral phase plate," IEEE Electron Device Lett. **35**(8), 856–858 (2014).
6. J. F. Algorri, V. Urruchi, N. Bennis, J. M. Sánchez-Pena, and J. M. Otón, "Tunable liquid crystal cylindrical micro-optical array for aberration compensation," Opt. Express **23**(11), 13899–13915 (2015).
7. J. F. Algorri, V. Urruchi, N. Bennis, and J. M. Sánchez-Pena, "A Novel High-Sensitivity, Low-Power, Liquid Crystal Temperature Sensor," Sensors (Basel) **14**(4), 6571–6583 (2014).
8. P. J. Pinzón, I. Pérez, C. Vázquez, and J. M. Sánchez Pena, "Reconfigurable 1×2 wavelength selective switch using high birefringence nematic liquid crystals," Appl. Opt. **51**(25), 5960–5965 (2012).
9. M. Ye, B. Wang, M. Uchida, S. Yanase, S. Takahashi, and S. Sato, "Focus tuning by liquid crystal lens in imaging system," Appl. Opt. **51**(31), 7630–7635 (2012).
10. Y.-H. Lin and M.-S. Chen, "A pico projection system with electrically tunable optical zoom ratio adopting two liquid crystal lenses," J. Disp. Technol. **8**(7), 401–404 (2012).
11. H.-C. Lin, N. Collings, M.-S. Chen, and Y.-H. Lin, "A holographic projection system with an electrically tuning and continuously adjustable optical zoom," Opt. Express **20**(25), 27222–27229 (2012).
12. Y.-S. Tsou, K.-H. Chang, and Y.-H. Lin, "A droplet manipulation on a liquid crystal and polymer composite film as a concentrator and a sun tracker for a concentrating photovoltaic system," J. Appl. Phys. **113**(24), 244504 (2013).

#296644 https://doi.org/10.1364/OE.25.014795
Journal © 2017 Received 24 May 2017; revised 11 Jun 2017; accepted 11 Jun 2017; published 19 Jun 2017

Optics EXPRESS

13. A. Hassanfiroozi, Y.-P. Huang, B. Javidi, and H.-P. D. Shieh, "Hexagonal liquid crystal lens array for 3D endoscopy," Opt. Express **23**(2), 971–981 (2015).
14. Pixeloptics, Adjustable electro-active optical system and uses thereof, US patent 20140204333 A1 (2014).
15. Y.-H. Lin and H.-S. Chen, "Electrically tunable-focusing and polarizer-free liquid crystal lenses for ophthalmic applications," Opt. Express **21**(8), 9428–9436 (2013).
16. D. W. Berreman, Variable-focus LC-lens system, Bell Telephone Laboratories, United States patent US 4190330, 1980.
17. S. Sato, "Liquid-crystal lens-cells with variable focal length," Jpn. J. Appl. Phys. **18**(9), 1679–1684 (1979).
18. T. Nose and S. Sato, "A liquid crystal microlens obtained with a non-uniform electric field," Liq. Cryst. **5**(5), 1425–1433 (1989).
19. J. F. Algorri, V. Urruchi, N. Bennis, J. M. Sánchez-Pena, and J. M. Otón, "Cylindrical Liquid Crystal Microlens Array with Rotary Optical Power and Tunable Focal Length," IEEE Electron Device Lett. **36**(6), 582–584 (2015).
20. G. Williams, N. Powell, A. Purvis, and M. G. Clark, "Electrically controllable liquid crystal fresnel lens," *In Opto-electronics Symposium SPIE* 1168 (1989).
21. G. D. Love and A. F. Naumov, "Modal liquid crystal lenses," Liq. Cryst. Today **10**(1), 1–4 (2000).
22. M. Y. Loktev, V. N. Belopukhov, F. L. Vladimirov, G. V. Vdovin, G. D. Love, and A. F. Naumov, "Wave front control systems based on modal liquid crystal lenses," Rev. Sci. Instrum. **71**(9), 3290–3297 (2000).
23. H. T. Dai, Y. J. Liu, X. W. Sun, and D. Luo, "A negative-positive tunable liquid-crystal microlens array by printing," Opt. Express **17**(6), 4317–4323 (2009).
24. H. Ren and S.-T. Wu, "Tunable electronic lens using a gradient polymer network liquid crystal," Appl. Phys. Lett. **82**(1), 22–24 (2003).
25. H. Ren, Y.-H. Lin, and S.-T. Wu, "Adaptive lens using liquid crystal concentration redistribution," Appl. Phys. Lett. **88**(19), 191116 (2006).
26. R. Rajasekharan, Q. Dai, H. Butt, K. Won, T. D. Wilkinson, and G. A. J. Amaratunga, "Optimization of nanotube electrode geometry in a liquid crystal media from wavefront aberrations," Appl. Opt. **51**(4), 422–428 (2012).
27. S.-H. Lin, L.-S. Huang, C.-H. Lin, and C.-T. Kuo, "Polarizer-free and fast response microlens arrays using polymer-stabilized blue phase liquid crystals," Appl. Phys. Lett. **96**(11), 113505 (2010).
28. H. Xianyu, S.-T. Wu, and C.-L. Lin, "Dual frequency liquid crystals: a review," Liq. Cryst. **36**(6-7), 717–726 (2009).
29. S. Qiong, *Fast Response Dual Frequency Liquid Crystal Materials*, Electronic Theses and Dissertations 4221, (2010). *http://stars.library.ucf.edu/etd/4221/*
30. H. K. Bücher, R. T. Klingbiel, and J. P. VanMeter, "Frequency-addressed liquid crystal field effect," Appl. Phys. Lett. **25**(4), 186–188 (1974).
31. M. Schadt, "Low-Frequency Dielectric Relaxations in Nematics and Dual-Frequency Addressing of Field Effects," Mol. Cryst. Liq. Cryst. (Phila. Pa.) **89**(1-4), 77–92 (1982).
32. Y.-H. Lin, J.-M. Yang, S.-T. Wu, C.-C. Liao, "Polarizer-free liquid crystal displays," *Optical Fiber Communication and Optoelectronics Conference 2007 Asia*, 31–33 (2007).
33. J. S. Hsu, B. J. Liang, and S. H. Chen, "Bistable chiral tilted-homeotropic nematic liquid crystal cells," Appl. Phys. Lett. **85**(23), 5511–5513 (2004).
34. X. Nie, T. X. Wu, Y.-Q. Lu, Y.-H. Wu, X. Liang, and S. T. Wu, "Dual-Frequency Addressed Infrared Liquid Crystal Phase Modulators with Submillisecond Response Time," Mol. Cryst. Liq. Cryst. (Phila. Pa.) **454**(1), 123–133 (2006).
35. X. Liang, Y.-Q. Lu, Y.-H. Wu, F. Du, H.-Y. Wang, and S.-T. Wu, "Dual-Frequency Addressed Variable Optical Attenuator with Submillisecond Response Time," Jpn. J. Appl. Phys. **44**(3), 1292–1295 (2005).
36. Y.-H. Fan, H. Ren, X. Liang, Y.-H. Lin, and S.-T. Wu, "Dual-frequency liquid crystal gels with submillisecond response time," Appl. Phys. Lett. **85**(13), 2451–2453 (2004).
37. O. Pishnyak, S. Sato, and O. D. Lavrentovich, "Electrically tunable lens based on a dual-frequency nematic liquid crystal," Appl. Opt. **45**(19), 4576–4582 (2006).
38. S. Suyama, M. Date, and H. Takada, "Three-Dimensional Display System with Dual-Frequency Liquid-Crystal Varifocal Lens," Jpn. J. Appl. Phys. **39**(1), 480 (2000).
39. Q. Song, M. Jiao, Z. Ge, H. Xianyu, S. Gauza, and S.-T. Wu, "High birefringence and low crossover frequency dual frequency liquid crystals," Mol. Cryst. Liq. Cryst. (Phila. Pa.) **488**(1), 179–189 (2008).
40. H. Xianyu, S. Gauza, and S.-T. Wu, "Sub-millisecond response phase modulator using a low crossover frequency dual-frequency liquid crystal," Liq. Cryst. **35**(12), 1409–1413 (2008).
41. J. F. Algorri, *Adaptive micro-optical phase modulators based on liquid crystal technology*, (2015), *http://e-archivo.uc3m.es/handle/10016/21765*.
42. D. Demus, J. Goodby, G. W. Gray, H.-W. Spiess, and V. Vill, *Physical Properties of Liquid Crystals* (WILEY-VCH Verlag GmbH, 2007).
43. G. Meier and A. Saupe, "Dielectric Relaxation in Nematic Liquid Crystals," Mol. Cryst. **1**(4), 515–525 (1966).
44. *Electrochemical Measurement System, Hardware Operator's Manual* (Gamry Instruments, 2005).
45. P. Kula, A. Aptacy, J. Herman, W. Wójciak, and S. Urban, "The synthesis and properties of fluoro-substituted analogues of 4-butyl-4′-[(4-butylphenyl)ethynyl]biphenyls," Liq. Cryst. **40**(4), 482–491 (2013).

Optics EXPRESS

46. P. Kula, J. Dziaduszek, J. Herman, and R. Dąbrowski, "9.4: Invited Paper: Highly Birefringent Nematic Liquid Crystals and Mixtures," *in SID Symposium Digest of Technical Papers*, 100–103 (2014).
47. R. Dąbrowski, P. Kula, and J. Herman, "High Birefringence Liquid Crystals," Crystals **3**(3), 443–482 (2013).
48. D. Węgłowsk, P. Kula, and J. Herman, "High birefringence bistolane liquid crystals: synthesis and properties," RSC Advances **6**(1), 403–408 (2016).
49. J. Herman and P. Kula, "Design of new super-high birefringent isothiocyanato bistolanes – synthesis and properties," Liq. Cryst. **0**, 1–6 (2017).
50. D. Ziobro, P. Kula, J. Dziaduszek, M. Filipowicz, R. Dąbrowski, J. Parka, J. Czub, S. Urban, and S. T. Wu, "Mesomorphic and dielectric properties of esters useful for formulation of nematic mixtures for dual frequency addressing system," Opto-Electron. Rev. **17**(1), 16–19 (2009).
51. V. Urruchi, J. F. Algorri, J. M. Sánchez-Pena, M. A. Geday, X. Quintana, and N. Bennis, "Lenticular Arrays Based on Liquid Crystals," Opto-Electron. Rev. **20**(3), 38–44 (2012).
52. H. Chen, M. Hu, F. Peng, J. Li, Z. An, and S.-T. Wu, "Ultra-low viscosity liquid crystal materials," Opt. Mater. Express **5**(3), 655–660 (2015).
53. F. Peng, F. Gou, H. Chen, Y. Huang, and S.-T. Wu, "A submillisecond-response liquid crystal for color sequential projection displays," J. Soc. Inf. Disp. **24**(4), 241–245 (2016).
54. S. Sato, "Applications of Liquid Crystals to Variable-Focusing Lenses," Opt. Rev. **6**(6), 471–485 (1999).

1. Introduction

Liquid crystals (LC) have been extensively used in numerous electro-optical devices. Fredericks effect makes the optical axis (director) align parallel to the electrical field. Liquid crystals are also anisotropic materials, having two different refractive indices in each axes. In consequence, by supplying a relatively low voltage, LC director is reoriented and the effective refractive index of the LC is modified. This effect, has been use not only in displays but also in optical phase modulators [1–6], thermometers [7], optical switches [8], etc. Particularly, LC lenses with tunable focal length by voltage, have shown many applications. This type of lenses, have the same applications than conventional fixed lenses, but with several advantages (small size, light weight, low driving voltages, low power consumption). For example, auto-focusing systems and optical zoom systems [9], pico-projection systems [10], correction of defects in a holographic projection system [11], photovoltaics [12] or bio-optics (endoscopy [13], ophthalmology [14,15]).

Since the first LC lens was proposed by Berreman et al. [16] and Sato et al. [17] several decades ago, a lot of different structures came up. Some of the most important are patterned electrodes [18,19], Fresnel lenses [20], modal control [21,22], immersed microlenses [23], etc. Another option is to modify the LC mixture itself. For example, polymer networks [24], concentration redistribution [25], carbon nanotubes [26], blue-phase LC [27], dual frequency LC [28], etc. This last option, is used to improve the switching time of the LC. Polymer networks and blue phases (a special cholesteric LC phase), have microsecond response time but the optical phase modulation is very limited.

Dual frequency liquid crystals (DFLCs) have a frequency revertible dielectric anisotropy. A DFLC mixture usually consists of two types of compounds: positive compounds, whose dielectric anisotropy ($\Delta\varepsilon$) is positive at low frequencies, but decreases as the driving frequency increases because of dielectric relaxation; and negative compounds, whose $\Delta\varepsilon$ is always negative and stays almost constant when the driving frequency is below the MHz range [29]. This effect, make it possible to align the molecular director by varying the frequency, instead of voltage [30, 31]. This kind of LC stem from the need of fast response time materials. Both the switching-on and off, are accelerated by applying different frequency signals. Until now, several devices has been proposed. For example displays (reflective displays [32] and bistable displays [33]) or photonics applications (optical phase modulators [34] attenuators [35], shutters [36], etc.). Tunable focus lenses made with this material, usually works in bistable mode [37,38], one frequency with positive dielectric anisotropy and another one with negative dielectric anisotropy, which makes the LC director and optical phase change with each frequency. One of the main drawbacks of DFLC was the high crossover frequencies, problems arising when high frequencies are applied (> 50 kHz) are higher cost in the driving circuit; larger heat dissipation; and stronger dielectric heating [29].

Optics EXPRESS

For this reason, the research on materials with low crossover frequencies led to novel materials [39,40].

In this work, we present a novel frequency dependent LC mixture for photonic applications, with emphasis on a LC microlens array. This mixture is a nematic composition of three different families of rodlike liquid crystals. All of the mixture components are dielectrically positive nematics or are dielectrically neutral. The key is that frequency dependence of parallel component of electric permittivity is different for each component. The result is that dielectric anisotropy is strongly dependent on frequency in one cases, whereas in others it is not. Combination of all components result to a frequency dependent positive nematic mixture. The novelty of this LC is a smooth and positive continuous dielectric anisotropy from a determined value to zero in more than two decades (100 Hz to 15 kHz). Moreover, the positive dielectric anisotropy in the whole range could be useful for some photonic applications.

The unique properties of this LC mixture are demonstrated to work in a frequency modulated LC microlens array. A hole patterned structure is used because it has a simple manufacturing process. Thanks to the special characteristics of this mixture, the microlenses are reconfigurable by low voltage signals with variable frequency. The result of this type of control are microlenses with low aberrations and fast switching times. The tunability with frequency and the fast switching, makes this liquid crystal of special interest not only for microlenses but for all kind of optical phase modulators with tunable capabilities.

2. Theoretical background

As it is commented in [41], the dependence of permittivity on the applied electric field frequency is known as dispersion. This physical effect is caused by the delay in molecular polarization with respect to an alternating electric field. The two different permittivities in a LC material usually have a different frequency-dependent response. The alternating electric field leads to a time lag between the average orientation of the dipole moment and the field. In general, the dipole moment is not along with the inertial axis of the molecule and there is a complicated relationship between the motion of the dipole, which determines the frequency of the permittivity, and the rotational motion of the molecule [42]. The ordinary parameter (ε_o) has a Debye type dispersion typical of fluids. This one usually occurs at microwave frequencies (>10^9Hz). The extraordinary parameter (ε_e) usually shows a lower frequency dispersion, in the radio frequency range. Some researchers as Meier [43] suggest that this dispersion could be caused by the dipolar moment relaxation; specifically, of the longitudinal axis of the molecule. The reorientation of this parameter by application of an electric field is hindered by a potential barrier owing to intermolecular forces. Most of the experimental observations, are explained by the three rotational movements (Fig. 1).

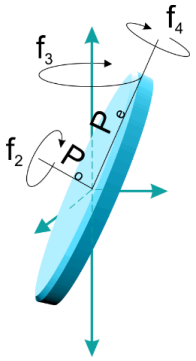

Fig. 1. Depiction of a LC molecule. The three relaxation modes for the rotational movement of the LC molecule related to three different frequencies (f_2, f_3, f_4).

Optics EXPRESS

The dipole moment (P) is split into two components parallel and perpendicular to the long molecular axis. This produces a typical frequency-dependent response (Fig. 2).

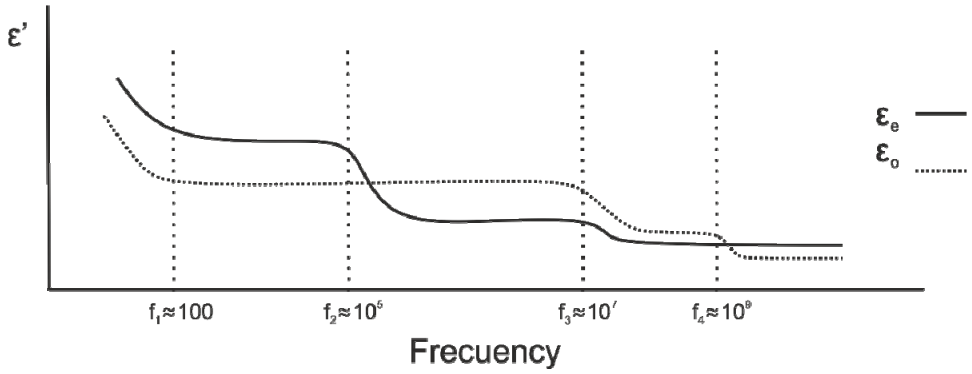

Fig. 2. Typical spectra of real permittivity (ordinary and extraordinary components) for nematic LC in a frequency range from 10Hz to 1GHz. Characteristic dispersion ranges.

The physical explanation for each zone is explained as follows:

1. For frequencies lower than f_1 ≈100 Hz the ions present in the LC contribute to the electric current, and so to the detected impedance.
2. The rotation around the short axes determines the permittivity response for frequencies lower than f_2 ≈100 kHz. As can be observed, this rotation only affects the behavior of the extraordinary component. The ordinary component is not hindered by the intermolecular forces.
3. The precession of long molecular axes are produced for a frequency of f_3 ≈10 MHz. Once this frequency is exceeded, the P_e contribution is reduced to a certain level. At the same time a Debye type dispersion is produced by the dipole moment P_o.
4. Finally, for frequencies higher than f_4 ≈1 GHz [43], only the fast rotation of molecules about long axes can follow the electric fields. From this frequency, the ordinary component, P_o, cannot follow this rotational movement while P_e contributes in the same way to ε_e.

In the proposed material, the rotation around the short axes occurs much before the typical frequency of 100 kHz, achieving a tunability with frequency in a workable range (frequencies lower than 10 kHz). In this case, the extraordinary component is going to zero while the ordinary component is not hindered by the intermolecular forces, achieving a tunable dielectric anisotropy from a determined value to zero. In order to demonstrate this effect, electrochemical impedance spectroscopy (EIS), is used.

In order to characterize LC by EIS some important issues have to be taken into account. The most important consideration is the use of low voltage electrical signals. In order to maintain linearity, it is recommended not to exceed 100 mV_{RMS}. Another requirement is the low resistance of the electrodes. Even, for high frequencies Au electrodes are recommended. The main reason is to avoid masking other effects by the own relaxation mode of the cell itself. The thickness can also affect the impedance. The analyzer Solartron 1260 has the frequency-impedance limit equal to $f \cdot Z < 10^9$ ΩHz [44]. Some capacitances can be masked by parasitic capacitances around the sample.

3. Liquid crystal mixture and structure

Investigated material is a nematic composition of three different families of rod like liquid crystals. Structures belong to fluorine substituted alkyl-alkyl phenyl-tolanes [45–47], Fig.

Optics EXPRESS

3(a), alkyl-alkyl bistolanes [48,49], Fig. 3(b), and fluorine substituted 4-[(4-cyanophenoxy)carbonyl]phenyl 4-alkylbenzoates [50], Fig. 3(c).

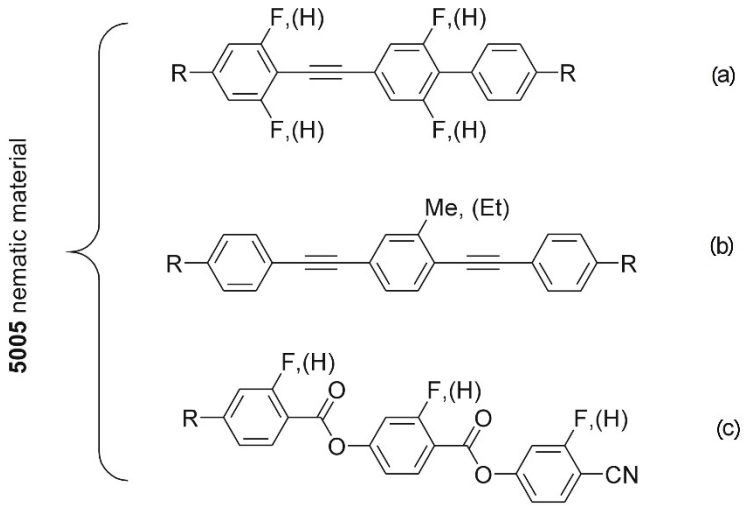

wherein R = alkyl = C_3H_7, C_4H_9, C_5H_{11}

Fig. 3. Components of 5005 nematic material. (a) Fluorine substituted alkyl-alkyl phenyl-tolanes, (b) alkyl-alkyl bistolanes and (c) fluorine substituted 4-[(4-cyanophenoxy)carbonyl]phenyl 4-alkylbenzoates.

All of the mixture components are dielectrically positive nematics (components a, c) or are dielectrically neutral (non polar compounds, b) but the frequency dependence of parallel component of electric permittivity for components (a) and (c) are different. For components (c) the dielectric anisotropy is strongly dependent on frequency and reduce its value from over hundred to close to zero for frequency much below 1 kHz, while for components a, up to MHz frequencies the dielectric anisotropy is weakly dependent. Combination of above mentioned compounds leads to a frequency dependent positive nematic mixture.

Two types of cells have been filled with this LC mixture. The first one, consists on monopixel cells to measure the electro-optical properties of LC. In this case, a continuous electrode in both substrates, having an active area of 1 cm^2 has been used. The thickness of measured cell was 10 μm. For the microlenses, a typical patterned structure with the hole array is designed and printed in a chrome photomask. The holes have a diameter of 100 μm and the distance between the adjacent holes is 10 μm. Two ITO coated substrates (20 Ω/sq) are photolithography etched as hole array electrode using this photomask. Prepared substrates were coated with polyimide alignment layer SE-130 (from Nissan Chemical Industries, Ltd.) for planar alignment, then mechanically buffed to define alignment direction for LC + molecules on the surface. Spacers of 40 μm diameter, mixed with optical glue, are deposited to separate the upper and bottom substrates. Finally, the experimental LC mixture (5005) fills the cavity.

4. Experimental set-up

The proposed device has to be characterized in several steps. The LC mixture is characterized electrically (to study the dielectric permittivity) and optically (to measure the switching time). Moreover, an optical set-up based on the interference of extraordinary and ordinary waveforms is used for the LC microlenses (to measure the optical phase modulation).

Optics EXPRESS

4.1 Dielectric anisotropy set-up

In order to measure the dielectric anisotropy, two parameters are firstly required, ordinary and extraordinary permittivity. In a cell with homogenous alignment, the LC director is parallel to the substrate when no voltage is applied, in this case, the electrical field is affected by the ordinary permittivity (short axis of the molecule, Fig. 1). When a voltage higher than the threshold voltage is applied, the molecule is aligned parallel to the electrical field (in case of positive dielectric anisotropy), in this case, the electrical field is affected by the extraordinary permittivity (long axis of the molecule, Fig. 1). In consequence, no voltage has to be applied to measure the ordinary permittivity in a homogenous cell. To measure the extraordinary permittivity there are two options: either make a homeotropic alignment (director perpendicular to the substrates) or align the LC molecules by voltage.

The ordinary permittivity has been measured by EIS (1260 Solartron impedance analyzer), applying a voltage of 100 mV_{RMS} and a frequency range from 100 Hz to 1 MHz. From the impedance measurements and knowing the structural parameters of the LC sample, the permittivity is estimated.

In order to measure the extraordinary permittivity, the two approaches commented before were tested. Making a homeotropic alignment was unsuccessful, due to the incapability of the molecules to arrange in such orientation after the filling process. After this, the second option was implemented by configuring the impedance meter with a special setup. As commented before, EIS requires sufficiently small voltage signals so that the system response is linear. In order to switch all the LC molecules, the voltage has to be much higher than the threshold voltage. In this case, at least more than 10 V_{RMS} is necessary to reach the saturation region. To solve this problem, and maintain the linearity of the system, the small AC signal probe has been set on a high bias (offset) DC voltage. One problem of LC materials when DC signals are applied, is the electrolytic degeneration of the LC cell by ion generation and migration, and eventual adsorption of the charges onto the alignment layers. To avoid this effect, the DC bias has been applied alternatively, with different polarity, during 1s. The result is that the DC voltage, is seen by the LC as a low frequency (0.5 Hz) AC square signal, with a root mean square value equal to the amplitude value (A) of the DC offset voltage. A depiction of this signal, in combination with the low amplitude AC signal, can be seen in Fig. 4. As the resulting signal has a square shape, the reorientation of the LC is not affected by polarity changes. Despite this, the sampling has been performed near the end of every cycle, to avoid possible transitional effects. Both data, from positive and negative half-cycles, have been collected independently. After a checking possible deviations one from another, there have not been observed any significant differences between them.

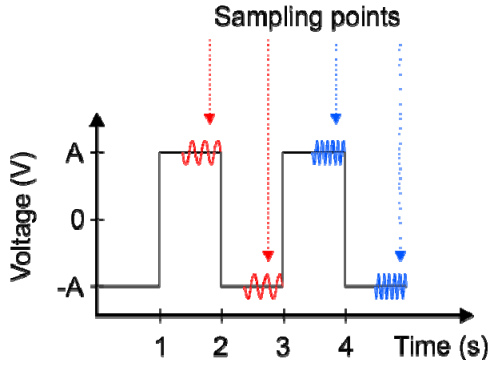

Fig. 4. Square driving waveform for impedance measurements. The small AC signal probe (red and blue signals) have been set on a high bias (offset) DC voltage (A is the DC offset). The result is that the DC voltage, is seen by the LC as a low frequency (0.5 Hz) AC square signal.

Optics EXPRESS

Several DC offsets has been tested, the result are square voltage signals with the following root mean square values, V_{RMS} = 0 V_{RMS}, 3 V_{RMS}, 8 V_{RMS}, 15 V_{RMS}. These values, correspond to voltages below the threshold, medium, and saturation levels, respectively. The low AC signal, is the same used in the previous experiment, sinusoidal voltage of 100 mV_{RMS} with a frequency range from 100 Hz to 1 MHz.

4.2 Switching time set-up

The switching time has been measured using radio frequency modulation techniques. In order to measure the time switching with voltage amplitude, an amplitude modulated (AM) signal is applied. The characteristics are, a 100% depth modulation from 0 to a variable voltage *V* and a frequency of 1 kHz. In the case of the frequency switching time, a frequency shift key (FSK) modulation from 40 kHz (mark frequency) to variable frequency *F* (space frequency), and fixed amplitude (4 V_{RMS}), is used. The time between modulations, are chosen to be long enough to completely commutate. Examples of these two configurations are depicted in Fig. 5.

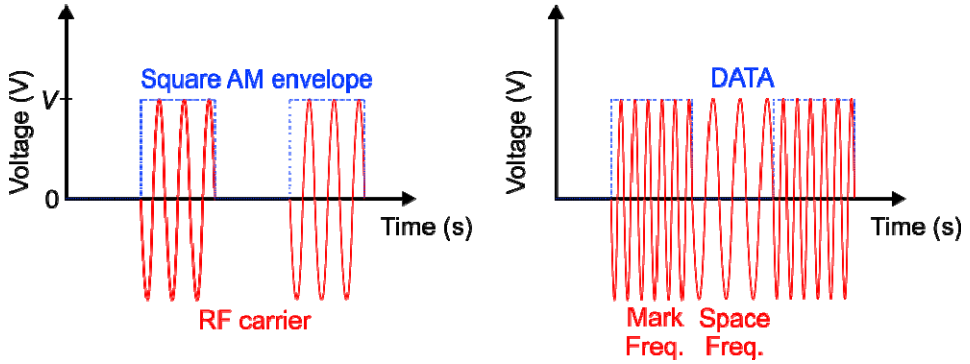

Fig. 5. (Left) Amplitude Modulation (AM) example. The characteristics are, a 100% depth modulation from 0 to a variable voltage V and a frequency of 1 kHz. (Right) Frequency Shift Key (FSK) signal example (two possible frequencies). Modulation from 40 kHz (mark frequency) to variable frequency F (space frequency), and fixed amplitude (4 V_{RMS}).

The LC monopixel cell is connected to a waveform generator (HP 33120A) with modulation capabilities. Then, the optical response is measured between crossed polarizers by a photodiode. This device converts optical intensity changes into voltage signals. Both voltages, from the waveform generator and photodiode are connected to an oscilloscope (SIGLENT SDS1064CFL).

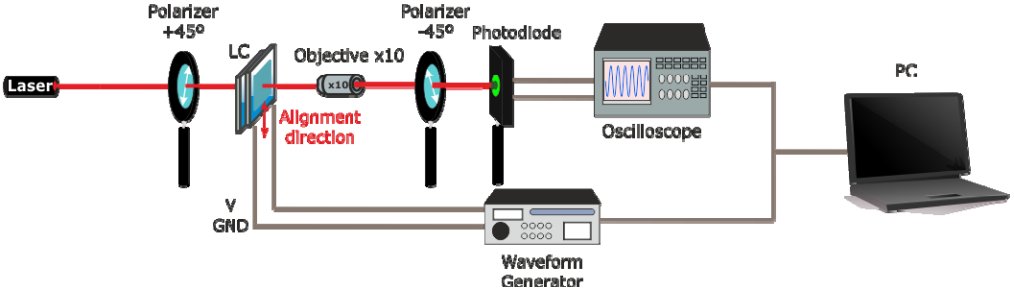

Fig. 6. Experimental set-up for characterizing the LC switching properties. The sample is placed between crossed polarizers.

The system is connected to a personal computer (PC). Considering the initial time as the change between signals (amplitude change in case of AM and frequency change in FSK), the

Optics EXPRESS

switching time is considered as the period of time between this first instant, and the 90% of the final intensity measured by the photodiode (Fig. 6).

4.3 Optical phase modulation set-up

In order to characterize the LC microlenses, the system is placed in an optical table as shown in Fig. 7. The experimental set-up is made of several optical components. The light source is a He-Ne laser (632.8nm), then a neutral density filters, a linear polarizer at + 45°, the LC cell with the alignment direction at 90°, a x10 microscope objective, a polarizer at −45° and a B/W CCD digital camera (Hamamatsu ORCA-ER, effective no. of pixels 1344 × 1024). All the angles have been referred to the horizontal direction of the optical table plane. The voltage is applied by means of a waveform generator (HP 33120A).

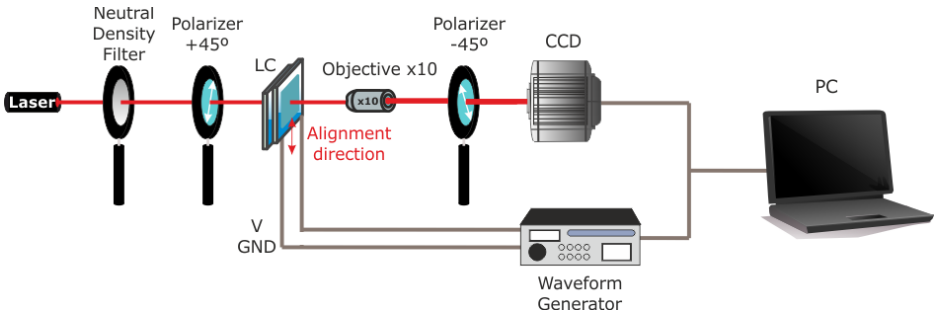

Fig. 7. Experimental set-up for characterizing tunable LC spherical microlens arrays. The sample is placed between crossed polarizers.

Both, the CCD and the waveform generator are connected to a PC. The resulting fringe patterns are recorded by a custom software programmed in MATLAB code. This program has an interface with several options to process the recorded image, for example: contrast improvements on fringe images, automatic rotations (when the device is at a specific angle), electrodes detection, area of interest selection, etc. Once the images from the CCD are processed, the program is capable of unwrapping the phase in 2D or 3D by Fringe Skeletonizing technique. The focal length can be also estimated following the process of [51].

5. Results

As indicated in previous sections, the results are grouped in three subsections. Firstly, the results of the dielectric anisotropy are shown. These results are fundamental in order to understand the electro-optical behavior of the LC microlenses. Secondly, the switching time of the LC is measured both, with amplitude control and frequency control. Finally, the electro-optical response of the LC microlenses is demonstrated, a tunable phase profile with frequency is shown.

5.1 Dielectric anisotropy

First of all, the impedance at 100 mV (ordinary axis of the LC molecules) is characterized by EIS. Then, as it was previously commented, a special set-up is used to measure the impedance of the extraordinary axis. From the impedance measurements and knowing the structural parameters of the LC sample, the permittivity is estimated. The results of the two experiments are shown in Fig. 8,

Optics EXPRESS

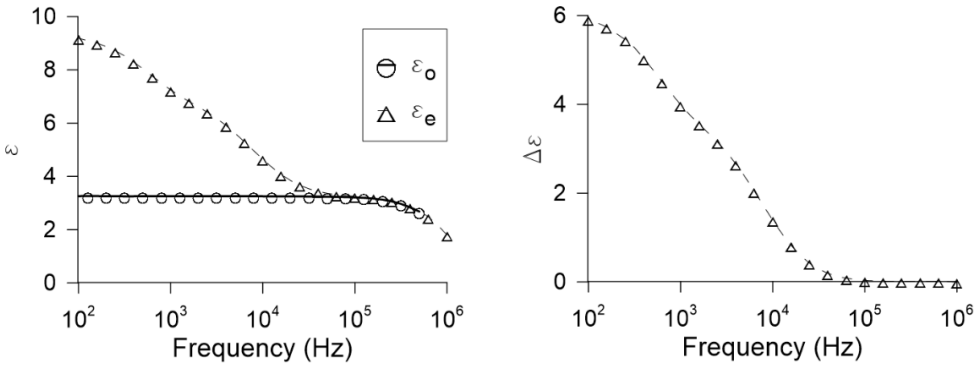

Fig. 8. (Left) Dispersion of the ordinary and extraordinary dielectric constants. (Right) dielectric anisotropy.

An unusual behavior is observed for the extraordinary permittivity. As can be seen in Fig. 2, the typical response of a nematic LC is a constant permittivity with frequency until 100 kHz - 1 MHz. In this case, the chemical composition of the LC, makes the extraordinary permittivity decreases until reach the ordinary permittivity value (Fig. 8, left). This effect, is produced for frequencies lower than 10 kHz. One possible explanation is that rotation around the short axes (Fig. 1) occurs much before the typical frequency of 100 kHz. This fact, produces a tunability of the extraordinary permittivity with frequency in a workable range (frequencies lower than 10 kHz). In this case, the extraordinary component is going to zero while the ordinary component is not hindered by the intermolecular forces, achieving a tunable dielectric anisotropy from a determined value to zero. Thanks to this, a complete tunability of the dielectric anisotropy (Fig. 8, right), from 6 to 0, is obtained. This tunability can be done with frequencies lower than 10 kHz. For this reason, optical phase modulation from 100 Hz to 10 kHz would be possible.

5.2 Switching time

Switching time is one of the most important parameters of LC. The decay time (T_{off}) is directly proportional on the thickness squared and the rotational viscosity, and inversely proportional to the elastic constant. In the case of the rise time (T_{on}), is directly proportional on the thickness squared and the rotational viscosity, and inversely proportional to the elastic constant and, the relation between the applied voltage and the threshold voltage, squared. For this reason, the decay time is usually a fixed value and higher than the rise time. Moreover, the rise time depend on the applied voltage. In this case, the decay time has been measured and it is 2 seconds for every case. The rise time, is measured following the set-up described in previous sections. Considering the switching time as the time when the 90% of the final optical transmission value is reached, the T_{on} is measured for the AM (1 kHz and variable voltage) and FSK (4 V_{RMS} and variable frequency) modulations. The result is shown in Fig. 9.

Optics EXPRESS

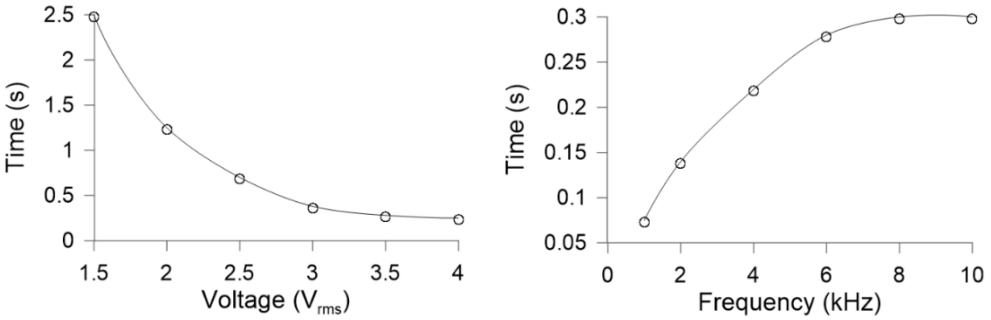

Fig. 9. Rise time for (left) 1 kHz and variable voltage and (right) 4 V_{RMS} and variable frequency.

As can be observed, the switching time with voltage amplitude is typical for a 10 µm cell (Fig. 9, left). Despite this, a considerable reduction on time is observed for the frequency modulation (Fig. 9, right). The frequency switching is around 10 times faster than amplitude modulation. As commented before, the switching time is directly proportional to the thickness squared, so for 1 µm cells, a submilisecond switching time (700 µs) with frequency control is expected, beyond the state of the art [52,53].

5.3 Electro-optical response of the LC microlenses

Firstly, a sinusoidal signal with variable amplitude and 1 kHz is applied to the control electrode of the LC microlenses. The results are shown in Fig. 10. The observed threshold voltage is high (compared to other commercial LC), lenses are not formed until 2 V_{RMS}. As can be seen, a typical astigmatic effect appears for the lowest voltages (there are more fringes in horizontal than vertical direction). This effect, is produced in the LC microlenses due to differences between the LC molecular alignment and the electrical field. The alignment of the molecules when the electrical field is parallel to the rubbing direction is considerably better than the opposite case. The literature suggest that this is caused by the difference between elastic constants [54]. The astigmatism coefficient tends to increase with increasing the ratio of the elastic constants (K33/K11). This aberration is higher for low voltages and almost disappear for higher voltages (4 V_{RMS} in this case). As most of the molecules are in perpendicular position, the effect of the alignment is considerable reduced. .

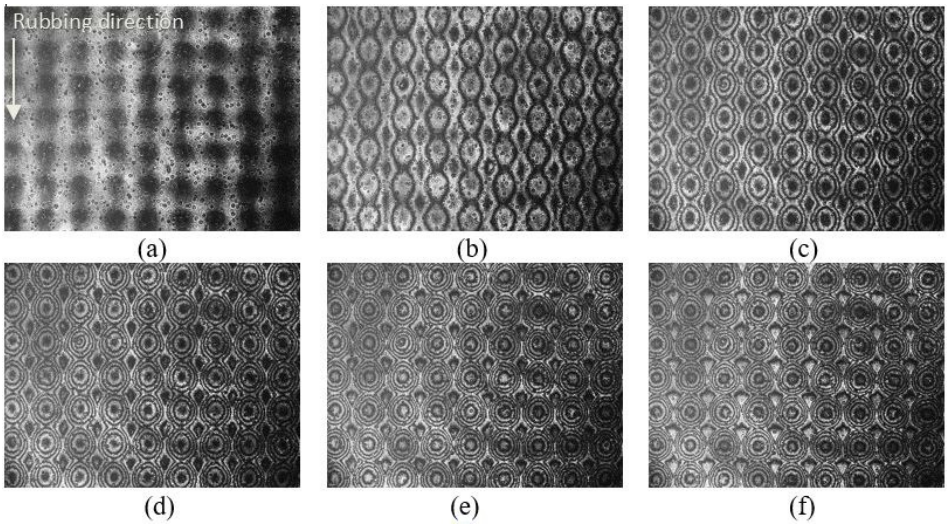

Fig. 10. Fringe patterns measured between crossed polarizers for (a) 1.5 V_{RMS}, (b) 2 V_{RMS}, (c) 2.5 V_{RMS}, (d) 3 V_{RMS}, (e) 3.5 V_{RMS}, (f) 4 V_{RMS}.

Optics EXPRESS

An interesting effect is observed when the frequency is modified. Common LC materials in a hole patterned configuration does not change the electro-optical response with frequency in a broad range (due to the permittivity response, Fig. 2). The dielectric dispersion occurs for very high frequencies (>100-500 kHz) so for lower frequencies the electric field distribution at the LC lens structure is not affected by it. With this new LC mixture, the LC lens profile can be frequency controlled in a very small range (from 1 kHz to 15 kHz). The reason was explained in section 5.1. As the dielectric anisotropy is tuned from 6 to 0, in this frequency range, the molecular director can be tuned with frequency. Figure 11, shows the fringe patterns for a sinusoidal signal with variable frequency and 4 V_{RMS}.

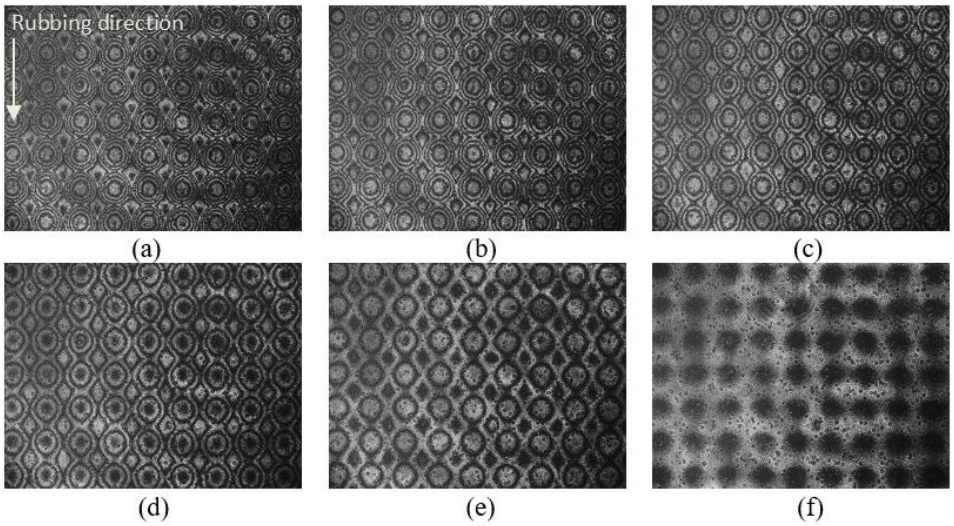

Fig. 11. Fringe patterns measured between crossed polarizers for (a) 2 kHz, (b) 4 kHz, (c) 6 kHz, (d) 8 kHz, (e) 10 kHz, (f) 15 kHz.

The most important thing is that astigmatism is considerably lower. As the driving voltage is always at $4V_{RMS}$ we do not have the problem caused by low voltage control. The mechanism of switching is different, for this reason the differences between elastic constant do not affect in the same way.

From the fringe patterns the phase profiles are extracted. The method is based on measuring the position of the fringes across the lens diameter. Two neighboring interference fringes have a phase difference of 2π. An image recognition program processes the images and plots phase retardation versus horizontal position across the LC microlens. The horizontal axis is taken as reference to plot the phase profiles. The results are shown in Fig. 12.

Optics EXPRESS

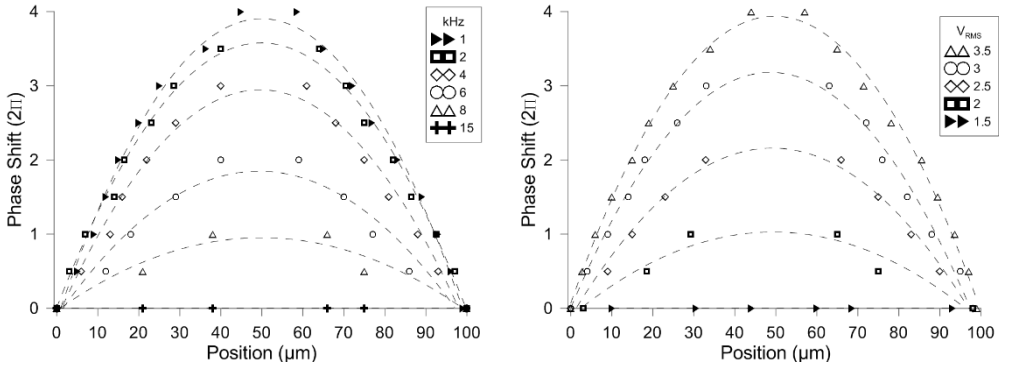

Fig. 12. Phase profiles for (left) frequency control, 4 V_{RMS} and variable frequency, and (right) voltage control, 1 kHz and variable voltage.

As can be observed, phase profiles can be controlled either by voltage or frequency. The focal length can be estimated by considering the number of fringes. This has been experimentally checked in [51]. The results are shown in Fig. 13.

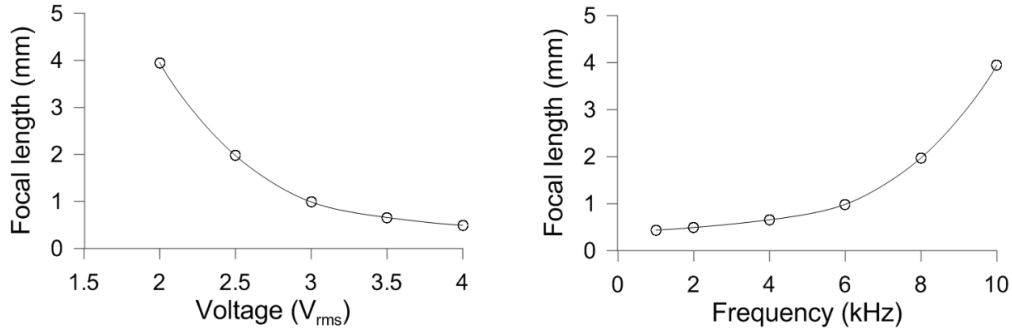

Fig. 13. Focal distance for (left) 1 kHz and variable voltage and (right) 4 V_{RMS} and variable frequency.

The focal length is tuned from 4 mm to 500 μm both with amplitude and frequency control. This is a first demonstration of a LC lens with tunable focal length by frequency in an analog way, to the best of our knowledge. Thanks to the tunable dielectric anisotropy of the LC, these microlenses have the advantages of fast switching and low aberrations. Moreover, this novel LC mixture could also work in other topologies and photonic devices with tunable phase modulation.

6. Conclusions

A novel liquid crystal (LC) mixture, is experimentally demonstrated to work in a LC spherical microlens array. This mixture is a nematic composition of three different families of rodlike liquid crystals. The key is that frequency dependence of parallel component of electric permittivity is different for each component, resulting in a strongly dependent on frequency dielectric anisotropy. The dielectric measurements reveal a complete tunability of the dielectric anisotropy from 6 to 0, with frequencies lower than 10 kHz. For this reason, optical phase modulation from 100 Hz to 10 kHz is possible. The switching time has been measured, both with voltage amplitude and frequency. The frequency switching is around 10 times faster than amplitude modulation. For 1 μm cells a submilisecond switching time (700 μs) with frequency control would be possible. The unique properties of this LC mixture are demonstrated to work in a frequency modulated LC microlens array. A hole patterned structure is used. Thanks to the special characteristics of this mixture, the microlenses are reconfigurable by low voltage signals with variable frequency. This is a first demonstration of

Optics EXPRESS

a LC lens with tunable focal length by frequency in an analog way. The most important thing is that astigmatism is considerably lower. As the driving voltage is always at $4V_{RMS}$ the problem caused by low voltage control is considerably reduced. The result of this type of control, are microlenses with low aberrations and fast switching. The tunability with frequency and the fast switching, makes this liquid crystal of special interest not only for microlenses but for all kind of optical phase modulators.

Funding

This work was supported by the Research and Development Program through the Comunidad de Madrid (SINFOTON S2013/MIT-2790), the Ministerio de Economía y Competitividad of Spain (TEC2013-47342-C2-2-R) and the funding from Agencia Estatal de Investigación (AEI) and Fondo Europeo de Desarrollo Regional (FEDER) for the Project TEC2016-77242-C3-1-R AEI/FEDER,UE. N Bennis and P Kula acknowledge the Polish Ministry of Science and Higher Education the Statutory Activity PBS-654 and PBS-651 of Military University of Technology respectively.